

# FiniteNet: A Fully Convolutional LSTM Network Architecture for Time-Dependent Partial Differential Equations

Ben Stevens<sup>1</sup> Tim Colonius<sup>1</sup>

## Abstract

In this work, we present a machine learning approach for reducing the error when numerically solving time-dependent partial differential equations (PDE). We use a fully convolutional LSTM network to exploit the spatiotemporal dynamics of PDEs. The neural network serves to enhance finite-difference and finite-volume methods (FDM/FVM) that are commonly used to solve PDEs, allowing us to maintain guarantees on the order of convergence of our method. We train the network on simulation data, and show that our network can reduce error by a factor of 2 to 3 compared to the baseline algorithms. We demonstrate our method on three PDEs that each feature qualitatively different dynamics. We look at the linear advection equation, which propagates its initial conditions at a constant speed, the inviscid Burgers' equation, which develops shockwaves, and the Kuramoto-Sivashinsky (KS) equation, which is chaotic.

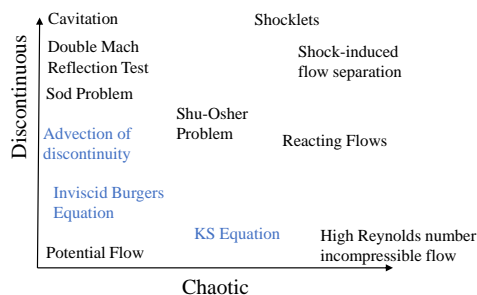
## 1. Introduction

### 1.1. Motivation

Partial differential equations (PDE) are fundamental to many areas of physics, such as fluid mechanics, electromagnetism, and quantum mechanics (Sommerfeld, 1949). All classical physics models are approximations obtained by coarse-graining the true quantum mechanical behavior of matter. For example, the Navier-Stokes equations are obtained by treating a fluid as a continuum; despite this, the equations are still too computationally expensive to solve for most practical problems (Ishihara et al., 2009), and so they are further coarse-grained by methods such as Large-Eddy Simulation (Halpern, 1993) or Reynolds Averaged Navier Stokes

(Chen et al., 1990) to infer sub-grid behavior. Each of these coarse-grained models save multiple orders of magnitude of computational expense (Drikakis & Geurts, 2006; Wilcox et al., 1998). However, these approaches do not lead to models that are generally applicable (Spalart, 2010).

PDEs give rise to vastly different solution structures in different problems (Sommerfeld, 1949). Hence, a solution approach that works well for one equation will not be generally applicable, as different difficulties can cause different methods to fail. The two major difficulties we examine in this paper are PDEs with chaotic dynamics, and PDEs with discontinuous solutions. PDEs with chaotic dynamics are challenging because small errors will grow quickly in time, causing the numerical solution to diverge from the true solution if the solver is not accurate enough (Strogatz, 2001). Typically, high-order numerical methods are used to solve these problems as they offer the best asymptotic error bounds (Deville et al., 2002). PDEs with discontinuous solutions are difficult to solve because high-order methods lead to Gibbs phenomena near discontinuities (Gottlieb & Shu, 1997), which can lead to numerical instabilities. High-order methods are derived with the assumption that the solution is smooth (LeVeque, 2007), but no method can achieve better than first-order accuracy in the presence of a discontinuity (LeVeque et al., 2002). Hence, we can see methods used to solve turbulence and discontinuities are at odds with each other, which makes it especially challenging to simulate problems with both of these issues. In 1.1, we present a qualitative overview of problems in fluid mechanics that involve turbulent and/or discontinuous solutions.



\*Equal contribution <sup>1</sup>Department of Mechanical and Civil Engineering, California Institute of Technology, Pasadena, CA, United States. Correspondence to: Ben Stevens <bstevens@caltech.edu>.

Figure 1. Problems with discontinuous and chaotic behavior. Problems in blue are examined in our experiments.

Numerical methods such as FDM and FVM are often developed without knowledge of the specific equation that they will be used to solve, and instead opt to maximize the rate of convergence (LeVeque, 2007). However, the dynamics of PDEs greatly influence the structure of their solutions. This information should be used to maximize the performance of the numerical methods used to simulate these equations. Machine learning is the natural tool to hybridize this information with traditional numerical methods, as detailed experimental/simulation data that contains this behavior is available and can be used to improve these numerical methods. Furthermore, machine learning techniques for capturing temporal behavior such as LSTMs (Hochreiter & Schmidhuber, 1997a;b; Gers et al., 1999), and spatially local behavior such as CNNs (Fukushima, 1980; LeCun et al., 1989; 1998), have undergone significant development. This makes machine learning highly effective for modeling problems with these structures, both of which occur in time-dependent PDEs.

## 1.2. Related Work

Research intersecting PDEs with ML can be divided into two main goals: discovering PDEs from data, and using ML to better solve PDEs (Raissi et al., 2019). Although our paper focuses on solving PDEs, we will briefly discuss efforts to discover them from data. Brunton et al. (2016) learned dynamical systems by applying lasso regression to a library of functions. Many papers used LSTMs or other sequence models to learn dynamical systems (Hagge et al., 2017; Yu et al., 2017; Vlachas et al., 2018; Wan et al., 2018; Li et al., 2017). Other papers learned coarse-graining models by following a system identification approach (Ling et al., 2016).

Solving PDEs with machine learning can be further broken up into two main areas: using data to develop better solvers, and parameterizing solutions to PDEs as a neural network and learning weights to minimize the pointwise error of the PDE (Lagaris et al., 1998). This second idea has been further developed (Rudd, 2013) to solve problems such as high-dimensional PDEs (Sirignano & Spiliopoulos, 2018). Hsieh et al. (2019) learned iterative PDE solvers for time-independent problems that are solved via matrix inversion. In our work, we focus on time-dependent problems that are solved via time-stepping, though both involve discretization. There have been numerous efforts to develop discretization methods tailored to specific types of dynamics. In fluid mechanics, much work has gone into developing shock capturing methods, spatial discretization algorithms specially suited towards solving PDEs with discontinuous solutions (Harten, 1983). This strategy can be viewed as a form of coarse-graining, as the true equations have viscous terms that prevent discontinuities from forming. They instead form very steep but continuous features, but these re-

quire a very fine grid to fully resolve. There have also been machine learning strategies that develop equation-specific spatial discretization schemes. The idea of embedding machine learning models into spatial discretization methods for the purpose of coarse-graining was introduced by Bar-Sinai et al. (2019). In their paper, they trained a neural network to interpolate over the solution of a PDE to more accurately predict the solution at the next timestep. PDE-Net followed a similar approach (Long et al., 2017; 2019) in learning derivatives while also learning the PDE from data.

## 1.3. Our Contribution

We try to simultaneously exploit the spatial and temporal structure of PDEs through the convolutional LSTM architecture of our neural network, while maintaining the computational structures used in FVM/FDM. While some papers use convolutional LSTMs or related architectures to predict future values of time-series that also possess the property of spatial locality (Mohan et al., 2019; Xingjian et al., 2015), none exploit the FVM/FDM structure that naturally discretize PDEs. Other papers have developed coarse-graining models by learning from data and have embedded these into CNNs (Bar-Sinai et al., 2019), but none simultaneously used an LSTM structure to also exploit the temporal structure of PDEs. We also present a novel training approach of directly minimizing simulation error over long time-horizons by building upon ideas developed for PDE-Net (Long et al., 2017). Our approach aims to push the field of data-driven scientific computing forward by combining these ideas in a sufficiently generic and efficient framework to permit extensions to many problems.

## 2. Numerical Methods Background

### 2.1. Strong Stability Preserving Runge-Kutta Methods

Runge-Kutta methods are a family of numerical integration methods used to advance a differential equation  $\frac{\partial u}{\partial t} = L(u)$  forward in time. In this paper, we use SSPRK3 (Gottlieb & Shu, 1998)

$$\begin{aligned} u^{(1)} &= u^{(n)} + \Delta t L(u^{(n)}), \\ u^{(2)} &= \frac{3}{4}u^{(n)} + \frac{1}{4}u^{(1)} + \frac{1}{4}\Delta t L(u^{(1)}), \\ u^{(n+1)} &= \frac{1}{3}u^{(n)} + \frac{2}{3}u^{(2)} + \frac{2}{3}\Delta t L(u^{(2)}), \end{aligned} \quad (1)$$

a three-step, third-order accurate method that preserves the total variation diminishing (TVD) property  $TV(u(t_{i+1})) \leq TV(u(t_i))$  of explicit Euler, where total variation is defined as

$$TV(u) = \sum_{i=1}^N |u(x_i) - u(x_{i-1})|. \quad (2)$$

A TVD method prevents the time-stepping method from adding spurious oscillations to the solution, which is a major concern for PDEs with discontinuous solutions, as they can lead to instabilities that crash the simulation in nonlinear PDEs such as the inviscid Burgers' equation.

## 2.2. Finite Difference Method

One spatial discretization method we combine with machine learning is FDM. In this method, derivatives of the solution are approximated as a weighted combination of local values of the solution. For example, one could approximate the first derivative of a function as

$$\frac{\partial u}{\partial x} \approx \frac{1}{\Delta x} \sum_{i=-1}^1 c_i u_i = \frac{u_1 - u_{-1}}{2\Delta x} \quad (3)$$

by using coefficients  $c_{-1} = -\frac{1}{2}$ ,  $c_0 = 0$ , and  $c_1 = \frac{1}{2}$ . We use the facts that the bounds on  $i$  can be expanded and the values of  $c_i$  are not fully constrained to allow a neural network to choose these coefficient values based on the local solution as  $c_{a:b} = f(u_{a:b})$ .

## 2.3. Finite Volume Method

We also consider equations that are more naturally solved using FVM, a spatial discretization method similar to FDM. FVM offers the advantage of improved stability (Bar-Sinai et al., 2019), and is easier to extend to unstructured meshes (Chen et al., 2003).

### 2.3.1. EXAMPLE

Consider the scalar conservation law

$$\frac{\partial u}{\partial t} + \frac{\partial f(u)}{\partial x} = 0 \quad (4)$$

One can split the  $x$ -domain into cells of width  $\Delta x$  and average over them as

$$\frac{1}{\Delta x} \int_{x_i}^{x_i+\Delta x} \frac{\partial u}{\partial t} + \frac{\partial f(u)}{\partial x} dx = 0 \quad (5)$$

to get

$$\frac{\partial \bar{u}_i}{\partial t} + \frac{f(u(x_i + \Delta x)) - f(u(x_i))}{\Delta x} = 0. \quad (6)$$

Note that this equation is still exact. The cell average values  $\bar{u}$  are tracked and interpolated to find  $u$  locally as

$$u(x_i) \approx \sum_{j=a}^b c_j \bar{u}_j. \quad (7)$$

Once again, the coefficients  $c_j$  are not fully constrained and can be determined using machine learning.

## 3. PDE Background

### 3.1. Advection Equation

The linear advection equation is written as

$$\frac{\partial u}{\partial t} + a \frac{\partial u}{\partial x} = 0. \quad (8)$$

It possesses solutions that are translations of the initial conditions at wavespeed  $a$ , i.e. for an initial condition of  $u(x, 0) = f(x)$ , the exact solution is  $u(x, t) = f(x - at)$ . In terms of coarse-graining, the sub-grid behavior has no influence on the solution at subsequent times. Once discretization occurs, no inference can be made about what happens between grid points, as this is fully determined by the initial condition rather than the dynamics of the equation. When this equation is solved with a discontinuous initial condition, it serves as a toy problem for advecting different materials in a multicomponent/multiphase flow. Numerical error causes the discontinuity to become smeared out during the simulation.

### 3.2. Inviscid Burgers' Equation

The inviscid Burgers' equation is written in non-conservative form as

$$\frac{\partial u}{\partial t} + u \frac{\partial u}{\partial x} = 0, \quad (9)$$

and is used to model wave-breaking. The nonlinear term causes shockwaves to form in finite time from smooth initial conditions. A shockwave is a special case of a discontinuity that is forced by the dynamics: unlike the linear advection equation, the discontinuity can propagate without progressive diffusion.

### 3.3. Kuramoto-Sivashinsky Equation

The KS equation is written as

$$\frac{\partial u}{\partial t} + \nu \frac{\partial^4 u}{\partial x^4} + \frac{\partial^2 u}{\partial x^2} + \frac{1}{2} \frac{\partial u^2}{\partial x} = 0, \quad (10)$$

and is used as a toy problem for turbulent flame fronts. Its dynamics lead to chaotic spatiotemporal behavior (Hyman & Nicolaenko, 1986). Chaos for PDEs is analogous to dynamical systems, defined by a small perturbation in initial conditions drastically affecting the time-evolution of the system (Strogatz, 2001).

## 4. Methodologies

### 4.1. Network Architecture

We structure our network to utilize well-known methods from numerical PDEs described earlier (SSPRK, FDM, and FVM). The network architecture mimics the structure of

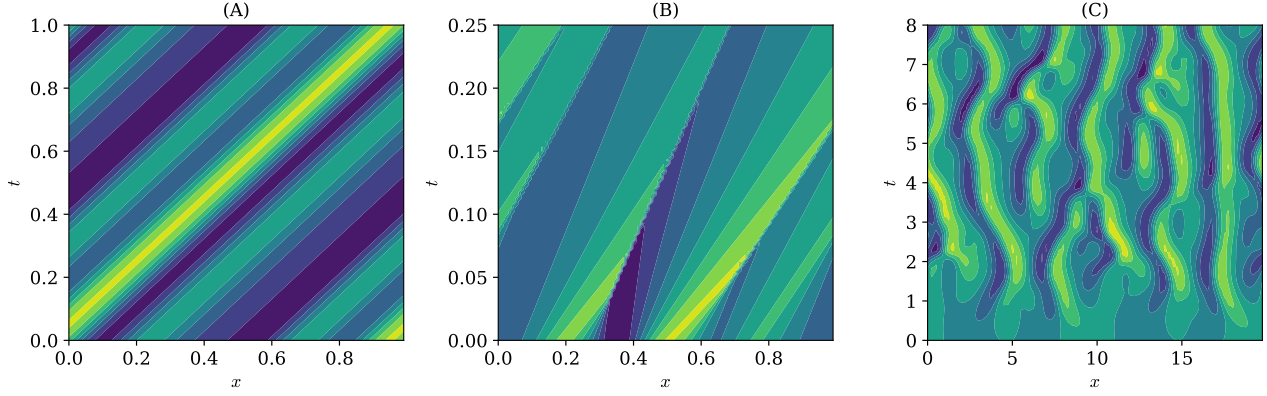


Figure 2. Example solution of (A) linear advection, (B) inviscid Burgers', and (C) KS equations

a grid used to numerically solve a PDE, where the size of the filter of the convolutional layer corresponds to the stencil that selects which information is used to compute the derivative, and each output of the network corresponds to the solution of the PDE at time  $t_j$  and location  $x_i$ . This can be seen in 4.1.

When looking at a specific realization of the stencil in the  $x$ -domain, we arrive at an LSTM network. The purpose of the LSTM is to transfer information about the solution over long time-horizons, which adds a feature to our method that is not present in traditional methods. The hidden information is transferred from substep to substep ( $t_{j-1}$  to  $t_{j-2/3}$  to  $t_{j-1/3}$ , and then to the next step at the end of the current step  $t_{j-1/3}$  to  $t_j$ ).

Within each evaluation of the LSTM, the information is used to compute the solution at the next substep in a way that mimics traditional FDM or FVM. The solution values at the previous timestep  $u_{i-2:i+2,j-1}$  and the hidden information with dimension 32 from the previous timestep are input to a neural network with 3 layers and 32 neurons per layer. This network outputs the hidden information to the next substep, as well as a prediction of the FVM or FDM coefficients. The neural network does not directly predict these coefficients. Instead, it first computes a perturbation  $\Delta \mathbf{c}$  to the maximum-order coefficients  $\mathbf{c}_{opt}$ , with  $l_2$  regularization applied to  $\Delta \mathbf{c}$ , similarly to a ResNet (He et al., 2016). We find that adding this step speeds up training and improves the performance of the model, as we are effectively biasing our estimate of the coefficients towards the coefficients that are optimal in the absence of prior knowledge about the solution. If the model is not confident about how perturbing  $\mathbf{c}_{opt}$  will affect the accuracy of the derivative it can output values close to zero to default back to  $\mathbf{c}_{opt}$ . Once  $\mathbf{c}_{opt}$  has been perturbed by  $\Delta \mathbf{c}$  to obtain  $\hat{\mathbf{c}}$ , an affine transformation is performed on  $\hat{\mathbf{c}}$  to guarantee that the coefficients are the desired order of

accuracy (Bar-Sinai et al., 2019). This is one of the main benefits of using an FDM structure for our model, as we can prove that our model gives a solution that converges to the true solution at a known rate as the grid is refined. The details of this transformation can be seen in section 4.3.

After the affine transformation, the final coefficients  $\mathbf{c}$  are known. The spatial derivatives are computed by taking the inner product of the coefficients  $c_{i-2:i+2}$  with  $u_{i-2:i+2,j-1}$ . For equations with multiple spatial derivatives, a different set of coefficients is computed for each. These spatial derivatives are then used to compute the time derivative, which can finally be used to compute the solution at the next substep. This process is then repeated for the desired number of timesteps. Our network architecture allows us to train on exact solutions or data of the PDE end-to-end.

## 4.2. Training Algorithm

We train our network in a way that exactly mimics how it would be used to solve a PDE. More specifically, we start with some random initial condition and use the network to step the solution forward in time, and compare the result to the exact solution. For the linear advection equation, the analytical solution is known for arbitrary initial conditions. For the inviscid Burgers' equation and KS equation, the same simulation is also carried out on a fine grid using a baseline numerical method, which results in a solution that can be considered approximately exact. The inviscid Burgers' equation is solved using WENO5 FVM (Jiang & Shu, 1996), and the KS equation is solved using fourth-order FDM. The loss is computed by downsampling the exact solution onto the grid of the neural network, averaging over the square error at every point in time and space. We found this training strategy to be far superior to training on only 1 time-step at a time, as our approach is capable of minimizing long-term error accumulation and training the network to be

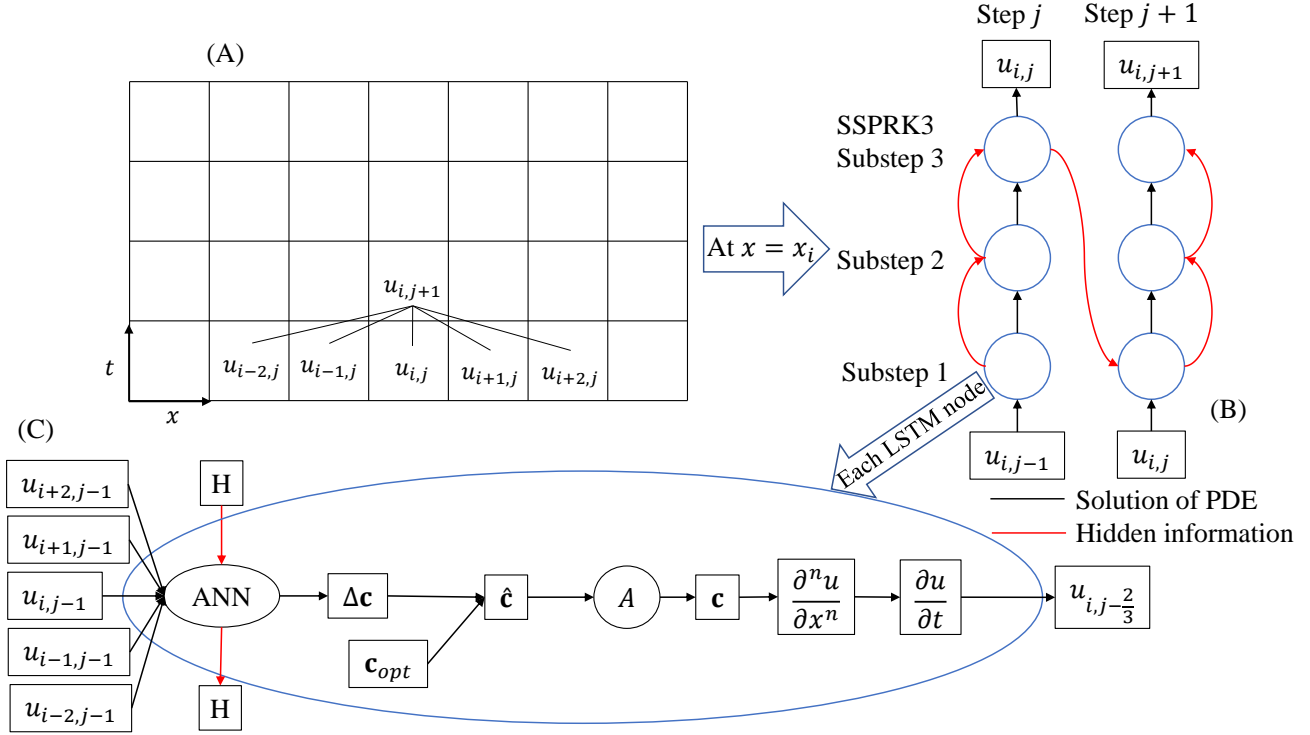


Figure 3. Network Architecture at (A) the top level, (B) LSTM at a specific  $x$  location, (C) each evaluation of the LSTM

numerically stable. In terms of computational complexity, our method is identical to backpropagation through time (BPTT) (Werbos, 1990).

### 4.3. Accuracy Constraints

FiniteNet is structured such that the numerical method is guaranteed to satisfy a minimum order of accuracy  $n$ ,  $e = o(\Delta x^n)$  (Bar-Sinai et al., 2019). One can perform a Taylor series expansion on the approximations of the form of 3 to obtain linear constraint equations that the coefficients must satisfy for the method to achieve a desired order of accuracy. We take the coefficients that the neural network outputs,  $\hat{\mathbf{c}}$ , and find the minimal perturbation  $\Delta \mathbf{c}$  that causes them to satisfy the constraint equations, which leads to the optimization problem

$$\begin{aligned} \min_{\Delta \mathbf{c} \in \mathbb{R}^5} \quad & \sum_{n=-2}^2 (\Delta c_n)^2 \\ \text{s.t.} \quad & A(\hat{\mathbf{c}} + \Delta \mathbf{c}) = \mathbf{b}, \end{aligned} \quad (11)$$

which has analytical solution  $\Delta \mathbf{c} = A^T(AA^T)^{-1}(\mathbf{b} - A\hat{\mathbf{c}})$ , which can be expressed as an affine transformation on  $\hat{\mathbf{c}}$ , and can therefore be added to the network as a layer with no activation function and untrainable weights.

## 5. Experimental Results

### 5.1. Summary

We find that our method is capable of reducing the error relative to the baseline method for all three equations tested. These results show promise for generalization to other equations, as each PDE we examined has qualitatively different behavior. A table summarizing our results can be seen in 1. The variation is due to averaging results from randomly generated initial conditions. The error ratio  $e_r$  is computed as  $e_r = \frac{e_F}{e_B}$  where  $e_F$  is the FiniteNet MSE and  $e_B$  is the MSE of the baseline method. We analyze  $\log_{10} e_r$  because  $\lim_{e_F \rightarrow 0} e_r \rightarrow 0$  and  $\lim_{e_B \rightarrow 0} e_r \rightarrow \infty$ . Hence, one case of the baseline method outperforming FiniteNet could skew the average and standard deviation of  $e_r$  significantly while the opposite would have very little effect, resulting in a bias. Additionally, the data empirically follows a log-normal distribution more closely than a normal distribution.

Hyperparameters were tuned to optimize performance on the linear advection equation. These same hyperparameters were then used as starting points for the other equations and tuned as necessary. For example, the time-horizon used in training was changed from 100 to 200 for the KS equation, as this helped FiniteNet track chaotic solutions over longer time-horizons. Additionally, it was found that increasing



**Algorithm 1** Train FiniteNet

```

Select number of epochs  $n_e$ 
Select minibatch size  $n_m$ 
Select time-horizon  $T$ 
for  $i = 1$  to  $n_e$  do
  Set total MSE to 0
  for  $j = 1$  to  $n_m$  do
    Select initial condition  $u_j(x, 0)$ 
    Determine exact solution  $u_j^*$ 
    Initialize hidden information  $H(0)$  to 0
    for  $k = 1$  to  $T$  do
      Compute  $u_j(x, t_k)$  and  $H(t_k)$  with FiniteNet
    end for
    Add MSE between  $u_j$  and  $u_j^*$  to total MSE
  end for
  Compute gradient of simulation error w.r.t. FiniteNet parameters
  Update FiniteNet parameters with ADAM optimizer
end for
    
```

Table 1. Mean and standard deviation of  $\log_{10} e_r$  for each PDE

EQUATION	$\log_{10} e_r$	BETTER?
LINEAR ADVECTION	$-0.27 \pm 0.08$	✓
INVISCID BURGERS'	$-0.53 \pm 0.08$	✓
KURAMOTO-SIVASHINSKY	$-0.62 \pm 0.41$	✓

the  $l_2$  regularization constant from  $\lambda = 0.001$  to  $0.1$  for the KS equations improved performance. The inviscid Burgers' equation was trained for 500 epochs instead of 400 because the error was still decreasing,

All data generation, training, and testing was carried out on a desktop computer with 32 GB of RAM and a single CPU with 3 GHz processing speed. Hence, by scaling the computing resources one could scale our method to more challenging problems. Our code and trained models can be found here: <https://github.com/FiniteNetICML2020Code/FiniteNet>, which includes links to our data.

We also find that FiniteNet trains methods that are stable, which tends to be a challenge in the field of learned FDM. Although we cannot formally prove stability, we observe in 5.1 that if the randomly initialized network weights lead to an unstable scheme, the method will quickly learn to become stable by minimizing accumulated error.

**5.2. Linear Advection Equation**

For the linear advection equation, we generate random discontinuous initial conditions, and compare the errors obtained using FiniteNet to errors obtained using WENO5. Each epoch involved generating 5 new initial conditions,

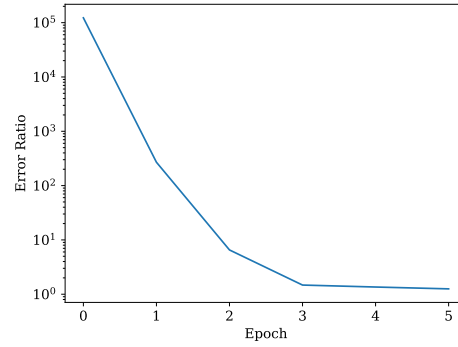


Figure 4. Training FiniteNet from unstable initial condition

computing the error against the exact solution, and updating the weights with the Adam optimizer (Kingma & Ba, 2014). We trained for 400 epochs.

After training was complete, we tested the model on 1000 more random initial conditions and computed the error ratio. We saw that FiniteNet outperformed WENO5 in 999 of the 1000 simulations. A PMF of the error ratio can be seen in 5.2.

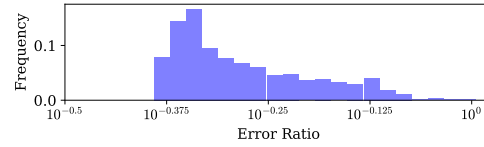


Figure 5. PMF of linear advection testing

We also plot a WENO5 solution and FiniteNet solution in 5.2 to gain insight into how FiniteNet improves the solution. We see that FiniteNet more sharply resolves discontinuities at the cost of adding oscillations, which leads to a net reduction in error.

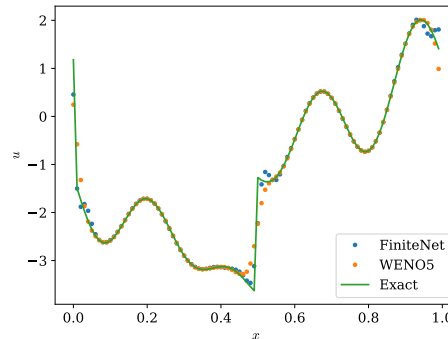


Figure 6. Solutions of linear advection equation

We can use this result to hypothesize that FiniteNet will further improve the solution when the discontinuity is larger. We verify our hypothesis by plotting error ratio against discontinuity width in 5.2, and verifying that larger discontinuities lead to lower error ratios.

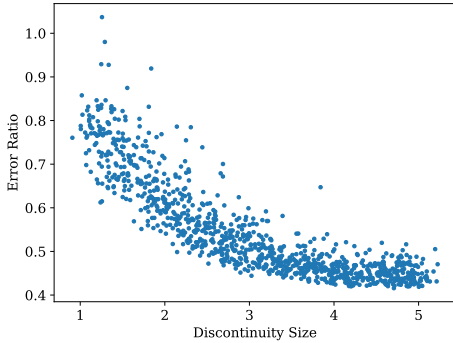


Figure 7. Discontinuity size vs error ratio for advection equation

### 5.3. Inviscid Burgers’ Equation

We train the neural network to interpolate flux values for the inviscid Burgers’ equation. Once again, each epoch involves generating five random initial conditions. In lieu of an exact solution, we use WENO5 on a 4x refined mesh to approximate the exact solution. We then ran 1000 simulations with the trained network and compared the results to WENO5. FiniteNet achieved a lower error on 998 of the 1000 test cases.

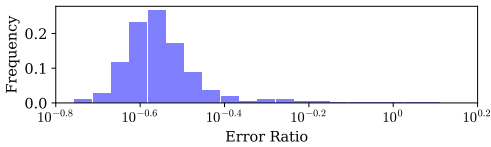


Figure 8. PMF of inviscid Burgers’ testing

By examining the error induced when numerically solving this equation with WENO5 and the FiniteNet, we see that WENO5 accumulates higher error around shocks. This tells us that FiniteNet achieves its error reduction by more sharply resolving the shocks.

We can get a prediction of roughly how many and how large of shocks will develop in the solution by looking at the total variation of the initial condition. We plot the total variation of the initial condition and compare it to the error ratio in 5.3.

This data shows that FiniteNet tends to do better relative to WENO5 when the total variation of the initial condition is higher, which helps confirm our result that FiniteNet offers

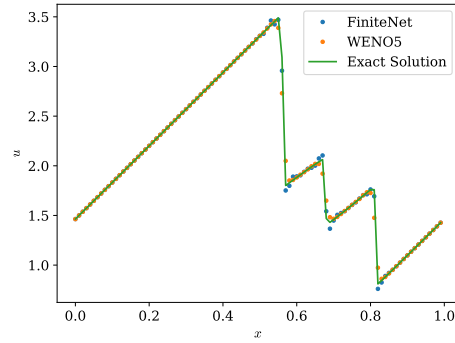


Figure 9. Solution of inviscid Burgers’ equation

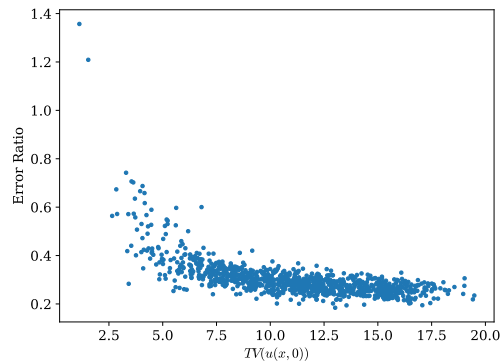


Figure 10. Trends between total variation and error ratio

the most improvement when many large shocks form.

### 5.4. Kuramoto-Sivashinsky Equation

The network is trained for the KS equation in the same way as was done for the inviscid Burgers’ equation: by solving the equation on a 4x refined mesh to closely approximate the exact solution. We generate our random initial conditions for training by setting a random initial condition for the exact solution and simulating until the trajectory has reached the chaotic attractor, and start training from random sequences of the solution on the attractor so that we are learning a more consistent set of dynamics, as the initial transient tends to be less predictable.

After training, we use both FiniteNet and fourth-order FDM to solve the KS equations from 1000 new initial conditions. We find the FiniteNet achieves a lower error in 961 of the 1000 tests. Interestingly, we see that in some cases standard FDM is unable to track the chaotic evolution and results in a solution with no visual fit, while FiniteNet succeeds at tracking the chaotic trajectory. In the cases where FiniteNet leads to a larger error than FDM, we see that neither method could track the chaotic trajectory, so there is some small

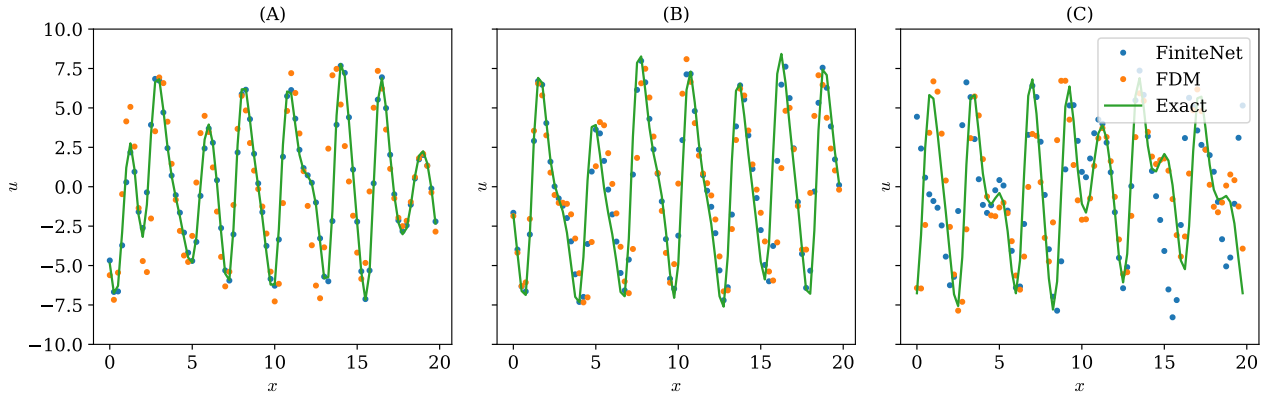


Figure 11. (A) Best case, (B) typical case, and (C) worst-case error ratio between FiniteNet and FDM for KS

probability that FiniteNet may follow a worse trajectory than FDM. In order to determine the reliability of FiniteNet compared to FDM, we compute the statistics of the errors individually. FiniteNet has mean error 1.20 and standard deviation 1.89, while FDM has mean error 2.94 and standard deviation 3.01. So we see that FDM error has higher mean and variance, and can conclude that FiniteNet is more reliable.

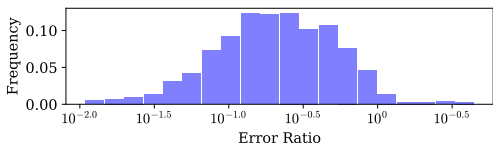


Figure 12. PMF of KS testing

## 6. Conclusions

In this paper, we have presented FiniteNet, a machine learning approach that can reduce the error of numerically solving a PDE. By combining the LSTM with well-understood and tested discretization schemes, we can significantly reduce the error for PDEs displaying a variety of behavior including chaos and discontinuous solutions. The FiniteNet architecture mimics the structure of a numerical PDE solver, and builds the timestepping method, spatial discretization, and PDE into the network. We train FiniteNet by using it to simulate the PDE, and minimizing simulation error against a trusted solution. This training approach causes the resulting numerical scheme to be empirically stable, which has been a challenge for other approaches.

We compared numerical solutions obtained by FiniteNet to those of baseline methods. We saw that for the inviscid Burgers’ equation and the linear advection equation,

FiniteNet is more sharply resolving discontinuities at the cost of sometimes adding small oscillations. This result makes intuitive sense, as the global error is dominated by regions near discontinuities so FiniteNet reduces the error the most by improving performance in these areas. When examining the KS equations, we see that FiniteNet reduces the error by more accurately tracking the chaotic trajectory of the exact solution. The main challenge of chaotic systems is that small errors grow quickly over time, which can lead to solutions that have completely diverged from the exact solution. FiniteNet is able to significantly reduce error by preventing this from happening in many realizations of this PDE.

Further work could involve comparing the runtime vs. error of FiniteNet to baseline approaches to more directly characterize how much of an improvement FiniteNet can offer. Additionally, we have till now only examined problems in one spatial dimension with periodic boundary conditions. It will be interesting to test the method on a large-scale problem, such as a turbulent flow.

## Acknowledgements

This material is based upon work supported by the National Science Foundation Graduate Research Fellowship under Grant No. 1745301

## References

Bar-Sinai, Y., Hoyer, S., Hickey, J., and Brenner, M. Learning data-driven discretizations for partial differential equations. *Proceedings of the National Academy of Sciences*, 116(31):15344–15349, 2019.

Brunton, S. L., Proctor, J. L., and Kutz, J. N. Discovering governing equations from data by sparse identification of



- nonlinear dynamical systems. *Proceedings of the national academy of sciences*, 113(15):3932–3937, 2016.
- Chen, C., Liu, H., and Beardsley, R. C. An unstructured grid, finite-volume, three-dimensional, primitive equations ocean model: application to coastal ocean and estuaries. *Journal of atmospheric and oceanic technology*, 20(1):159–186, 2003.
- Chen, H., Patel, V., and Ju, S. Solutions of reynolds-averaged navier-stokes equations for three-dimensional incompressible flows. *Journal of Computational Physics*, 88(2):305–336, 1990.
- Deville, M. O., Fischer, P. F., Fischer, P. F., Mund, E., et al. *High-order methods for incompressible fluid flow*, volume 9. Cambridge university press, 2002.
- Drikakis, D. and Geurts, B. *Turbulent flow computation*, volume 66. Springer Science & Business Media, 2006.
- Fukushima, K. Neocognitron: A self-organizing neural network model for a mechanism of pattern recognition unaffected by shift in position. *Biological cybernetics*, 36(4):193–202, 1980.
- Gers, F. A., Schmidhuber, J., and Cummins, F. Learning to forget: Continual prediction with lstm. 1999.
- Gottlieb, D. and Shu, C.-W. On the gibbs phenomenon and its resolution. *SIAM review*, 39(4):644–668, 1997.
- Gottlieb, S. and Shu, C.-W. Total variation diminishing runge-kutta schemes. *Mathematics of computation of the American Mathematical Society*, 67(221):73–85, 1998.
- Hagge, T., Stinis, P., Yeung, E., and Tartakovsky, A. M. Solving differential equations with unknown constitutive relations as recurrent neural networks. *arXiv preprint arXiv:1710.02242*, 2017.
- Halpern, B. *Large eddy simulation of complex engineering and geophysical flows*. Cambridge University Press, 1993.
- Harten, A. High resolution schemes for hyperbolic conservation laws. *Journal of computational physics*, 49(3):357–393, 1983.
- He, K., Zhang, X., Ren, S., and Sun, J. Deep residual learning for image recognition. In *Proceedings of the IEEE conference on computer vision and pattern recognition*, pp. 770–778, 2016.
- Hochreiter, S. and Schmidhuber, J. Long short-term memory. *Neural computation*, 9(8):1735–1780, 1997a.
- Hochreiter, S. and Schmidhuber, J. Lstm can solve hard long time lag problems. In *Advances in neural information processing systems*, pp. 473–479, 1997b.
- Hsieh, J.-T., Zhao, S., Eismann, S., Mirabella, L., and Ermon, S. Learning neural pde solvers with convergence guarantees. *arXiv preprint arXiv:1906.01200*, 2019.
- Hyman, J. M. and Nicolaenko, B. The kuramoto-sivashinsky equation: a bridge between pde’s and dynamical systems. *Physica D: Nonlinear Phenomena*, 18(1-3):113–126, 1986.
- Ishihara, T., Gotoh, T., and Kaneda, Y. Study of high-reynolds number isotropic turbulence by direct numerical simulation. *Annual Review of Fluid Mechanics*, 41:165–180, 2009.
- Jiang, G. and Shu, C. Efficient implementation of weighted eno schemes. *Journal of computational physics*, 126(1):202–228, 1996.
- Kingma, D. and Ba, J. Adam: A method for stochastic optimization. *arXiv preprint arXiv:1412.6980*, 2014.
- Lagaris, I., Likas, A., and Fotiadis, D. Artificial neural networks for solving ordinary and partial differential equations. *IEEE transactions on neural networks*, 9(5):987–1000, 1998.
- LeCun, Y., Boser, B., Denker, J. S., Henderson, D., Howard, R. E., Hubbard, W., and Jackel, L. D. Backpropagation applied to handwritten zip code recognition. *Neural computation*, 1(4):541–551, 1989.
- LeCun, Y., Bottou, L., Bengio, Y., and Haffner, P. Gradient-based learning applied to document recognition. *Proceedings of the IEEE*, 86(11):2278–2324, 1998.
- LeVeque, R. J. *Finite difference methods for ordinary and partial differential equations: steady-state and time-dependent problems*, volume 98. Siam, 2007.
- LeVeque, R. J. et al. *Finite volume methods for hyperbolic problems*, volume 31. Cambridge university press, 2002.
- Li, Y., Yu, R., Shahabi, C., and Liu, Y. Diffusion convolutional recurrent neural network: Data-driven traffic forecasting. *arXiv preprint arXiv:1707.01926*, 2017.
- Ling, J., Kurzawski, A., and Templeton, J. Reynolds averaged turbulence modelling using deep neural networks with embedded invariance. *Journal of Fluid Mechanics*, 807:155–166, 2016.
- Long, Z., Lu, Y., Ma, X., and Dong, B. Pde-net: Learning pdes from data. *arXiv preprint arXiv:1710.09668*, 2017.
- Long, Z., Lu, Y., and Dong, B. Pde-net 2.0: Learning pdes from data with a numeric-symbolic hybrid deep network. *Journal of Computational Physics*, 399:108925, 2019.

- Mohan, A., Daniel, D., Chertkov, M., and Livescu, D. Compressed convolutional lstm: An efficient deep learning framework to model high fidelity 3d turbulence. *arXiv preprint arXiv:1903.00033*, 2019.
- Raissi, M., Perdikaris, P., and Karniadakis, G. E. Physics-informed neural networks: A deep learning framework for solving forward and inverse problems involving nonlinear partial differential equations. *Journal of Computational Physics*, 378:686–707, 2019.
- Rudd, K. *Solving partial differential equations using artificial neural networks*. PhD thesis, Duke University, 2013.
- Sirignano, J. and Spiliopoulos, K. Dgm: A deep learning algorithm for solving partial differential equations. *Journal of Computational Physics*, 375:1339–1364, 2018.
- Sommerfeld, A. *Partial differential equations in physics*. Academic press, 1949.
- Spalart, P. Reflections on rans modelling. In *Progress in Hybrid RANS-LES Modelling*, pp. 7–24. Springer, 2010.
- Strogatz, S. *Nonlinear dynamics and chaos: with applications to physics, biology, chemistry, and engineering (studies in nonlinearity)*. 2001.
- Vlachas, P. R., Byeon, W., Wan, Z. Y., Sapsis, T. P., and Koumoutsakos, P. Data-driven forecasting of high-dimensional chaotic systems with long short-term memory networks. *Proceedings of the Royal Society A: Mathematical, Physical and Engineering Sciences*, 474(2213): 20170844, 2018.
- Wan, Z. Y., Vlachas, P., Koumoutsakos, P., and Sapsis, T. Data-assisted reduced-order modeling of extreme events in complex dynamical systems. *PloS one*, 13(5), 2018.
- Werbos, P. J. Backpropagation through time: what it does and how to do it. *Proceedings of the IEEE*, 78(10):1550–1560, 1990.
- Wilcox, D. C. et al. *Turbulence modeling for CFD*, volume 2. DCW industries La Canada, CA, 1998.
- Xingjian, S., Chen, Z., Wang, H., Yeung, D.-Y., Wong, W.-K., and Woo, W.-c. Convolutional lstm network: A machine learning approach for precipitation nowcasting. In *Advances in neural information processing systems*, pp. 802–810, 2015.
- Yu, R., Zheng, S., Anandkumar, A., and Yue, Y. Long-term forecasting using tensor-train rnns. *Arxiv*, 2017.